



Italian National Agency for New Technologies,
Energy and Sustainable Economic Development

ANALYSES OF AN UNMITIGATED STATION BLACKOUT TRANSIENT WITH ASTEC, MAAP AND MELCOR CODE

9th Meeting of the “European MELCOR User Group”, Madrid, Spain, April 6-7, 2017

F. Mascari¹, J. C. De La Rosa Blul², M. Sangiorgi², Giacomino Bandini¹

¹ENEA, Via Martiri di Monte Sole 4, 40129, Bologna, Italy

²European Commission, Joint Research Centre, Directorate G - Nuclear Safety and Security - Nuclear Reactor Safety & Emergency Preparedness, Westerduinweg 3, Postbus Nr. 2, 1755 ZG Petten (N.-H.) – Netherlands



1101 0110 1100
0101 0010 1101
0001 0110 1110
1101 0010 1101
1111 1010 0000



CONTENTS

- ENEA AND JRC JOINT ACTIVITY IN THE EU CESAM PROJECT - WP40-SAM
- SBO TRANSIENT INVESTIGATED
- CODE APPLICATION: PWR NODALIZATION DESCRIPTION
- CODE APPLICATION : PWR STEADY STATE ANALYSES
- CODE APPLICATION: TRANSIENT ANALYSES
- CONCLUSIONS

ENEA AND JRC JOINT ACTIVITY IN THE EU CESAM PROJECT - WP40-SAM

- ❑ In the framework of the European Project CESAM (**Code for European Severe Accident Management**) **WP40-SAM**, ENEA is involved in the development of a “PWR 900 like” with MELCOR code for benchmarking ASTEC code.

- ❑ **Within this CESAM framework, ENEA and JRC started a joint research activity** focused on the analysis of an unmitigated Station Blackout (SBO) with MELCOR (analyses developed by ENEA) and MAAP (analyses developed by JRC) code in order to benchmark ASTEC code (analyses developed by JRC).

- ❑ The references used to develop the “PWR900 like” MELCOR nodalization are :
 - *L. FOUCHER, ASTEC V20R3, “PWR900 like” ASTEC Input Deck, Rapport n PSN-RES/SAG/2013-451.*
 - *L. FOUCHER, ASTEC V20R3, “PWR900 like” ASTEC Steady state calculation, Rapport n PSN-RES/SAG/2013-466.*

SBO TRANSIENT MAIN CHARACTERISTICS

- ❑ The activity is focused on the use of **MAAP** and **MELCOR code** to simulate an *“Unmitigated Station Black-Out (SBO)”* to benchmark **ASTEC code**.

- ❑ The SBO transient is unmitigated and the Start Of the Transient (SOT) is characterized by:
 - **Loss of offsite Alternating Current (AC) power:**
 - **Failure of all the diesel generators;**

Therefore:

- **PRZ level control is unavailable;**
- **RCP seal injection is unavailable;**
- **Active safety injection systems are unavailable;**
- **Motor-driven Auxiliary Feedwater (MDAFW) system is unavailable;**
- **Auxiliary feed water is unavailable.**

SBO TRANSIENT MAIN CHARACTERISTICS

- ❑ At the SOT, the following events take place:
 - SCRAM;
 - Main Steam Isolation Valves (MSIVs) closure;
 - Main Feed Water closure;
 - Start of the pump coast-down.

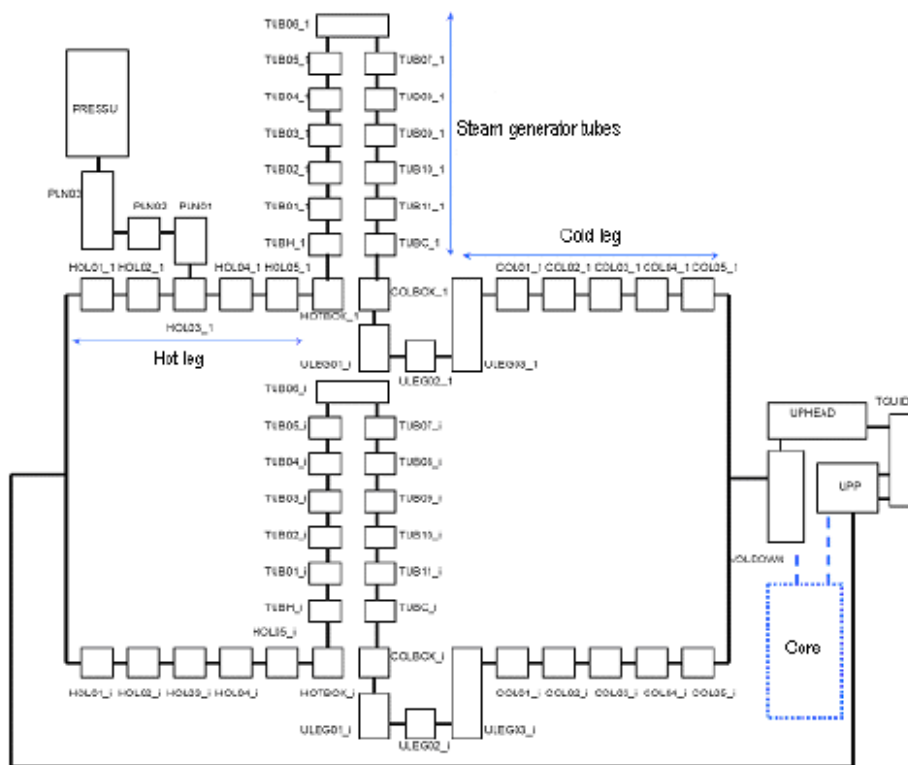
- ❑ For this first analysis the following hypotheses are also considered:
 - Independent failure of the Turbine Driven Auxiliary Feedwater (TDAFW) pump;
 - No Reactor Coolant Pump (RCP) seals failure;
 - Independent failure of the accumulators;
 - No primary boundary structures thermal induced degradation phenomena (SGTR not considered, HL/surge line creep rupture not considered)
 - Station battery is always in operation;
 - Post core damage strategy is assumed (SEBIM manually stuck open when the core exit temperature -CET- reaches 650 °C).

CODE NODALIZATIONS: Volumes Comparison

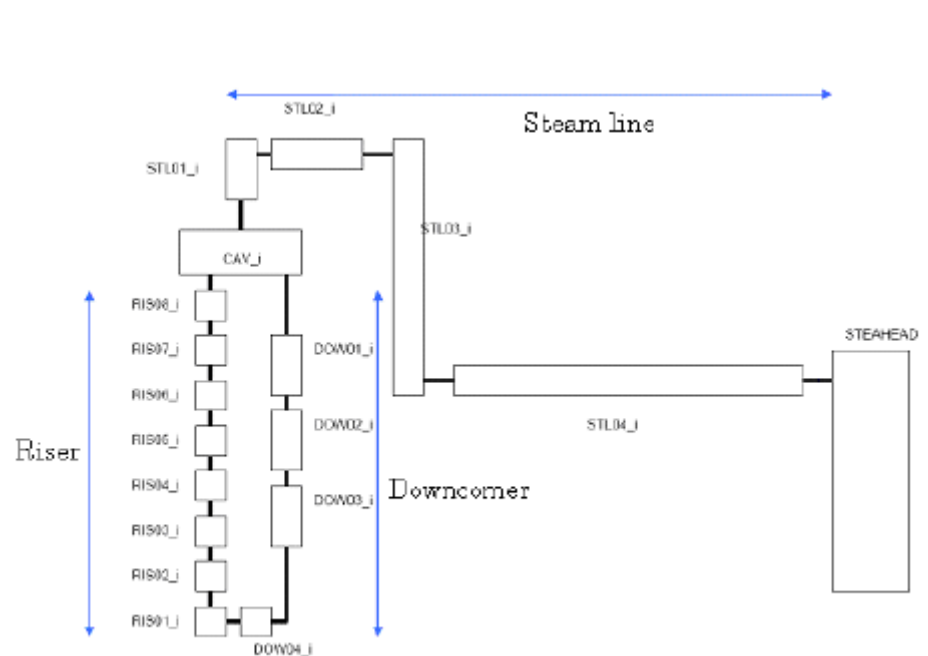
Volume (m ³)	ASTEC		MAAP	MELCOR	
Primary Side Loop					
HL	2.75		2.75	2.75	
Water box SG Hot Side	5.48	33.23	33.23	16.98	33.23
SG Ascending Side	10.38				
TOP U Tube	2.24			-	
SG Descending Side	10.38				
SG Water Box Cold Side	4.75			16.25	
Loop Seal	5.14		5.14	5.14	
CL	7.674		7.674	7.674	
Surge Line	1.352		*	1.352	
PRZ	42.42		42.42	42.42	
Secondary Side					
SG Riser	75.75	151.43	-	151.43	
Cavity	75.68		-		
SG DC	24.47		-	24.47	
TOT SG	175.94		-	175.94	



CODE NODALIZATIONS: ASTEC Plant Model Description



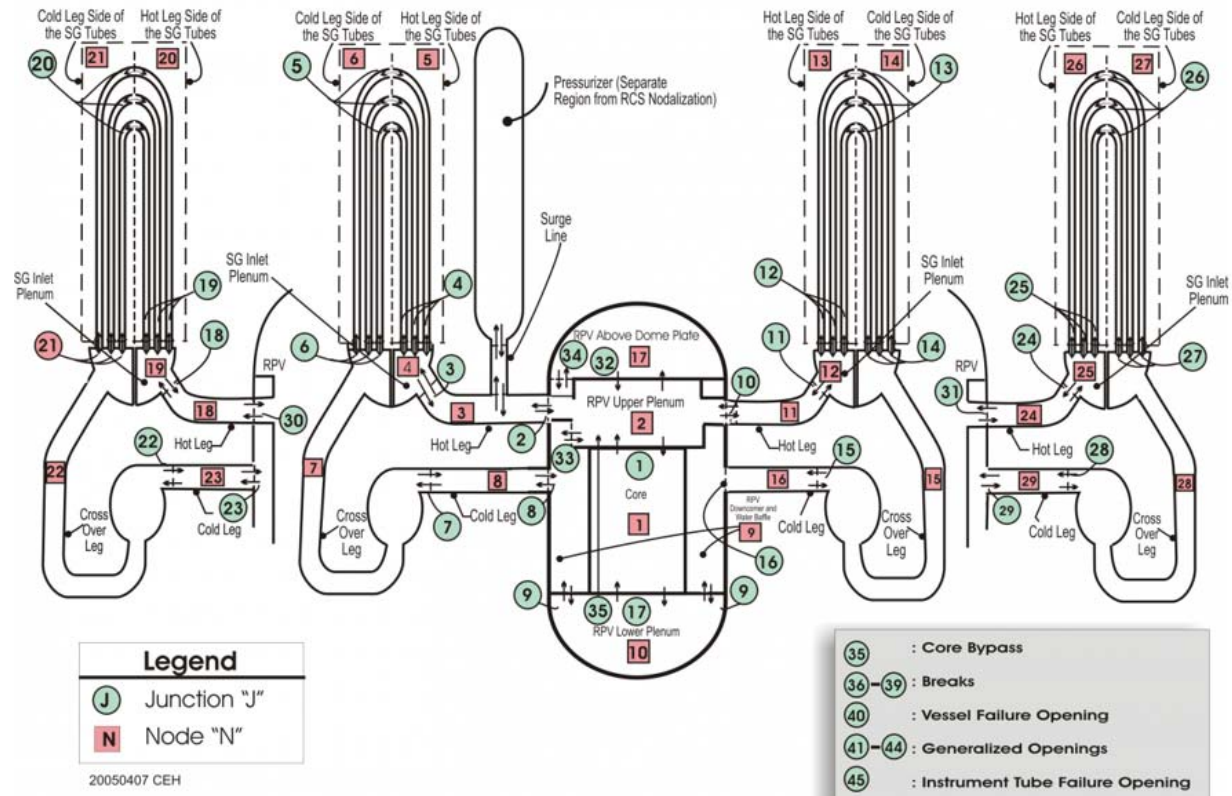
ASTEC nodalization of the primary circuit



ASTEC nodalization of the secondary circuit

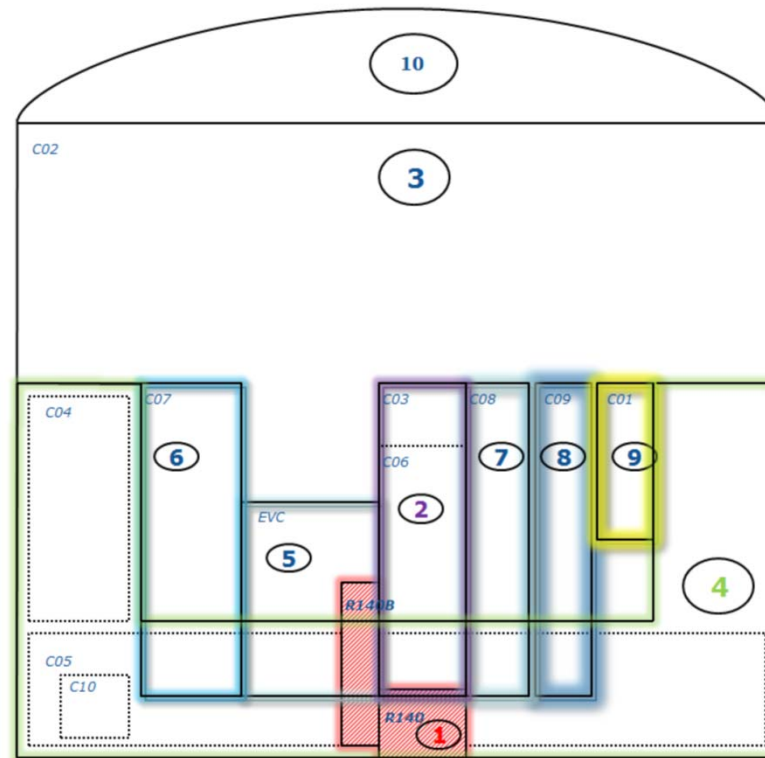


CODE NODALIZATIONS: MAAP Plant Model Description

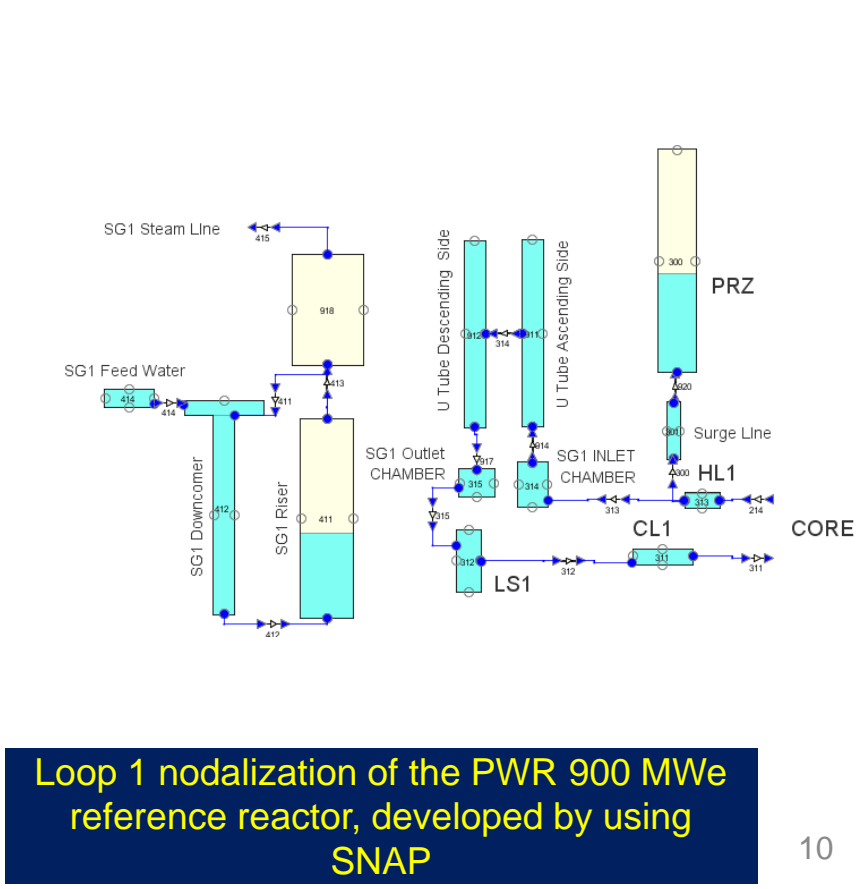
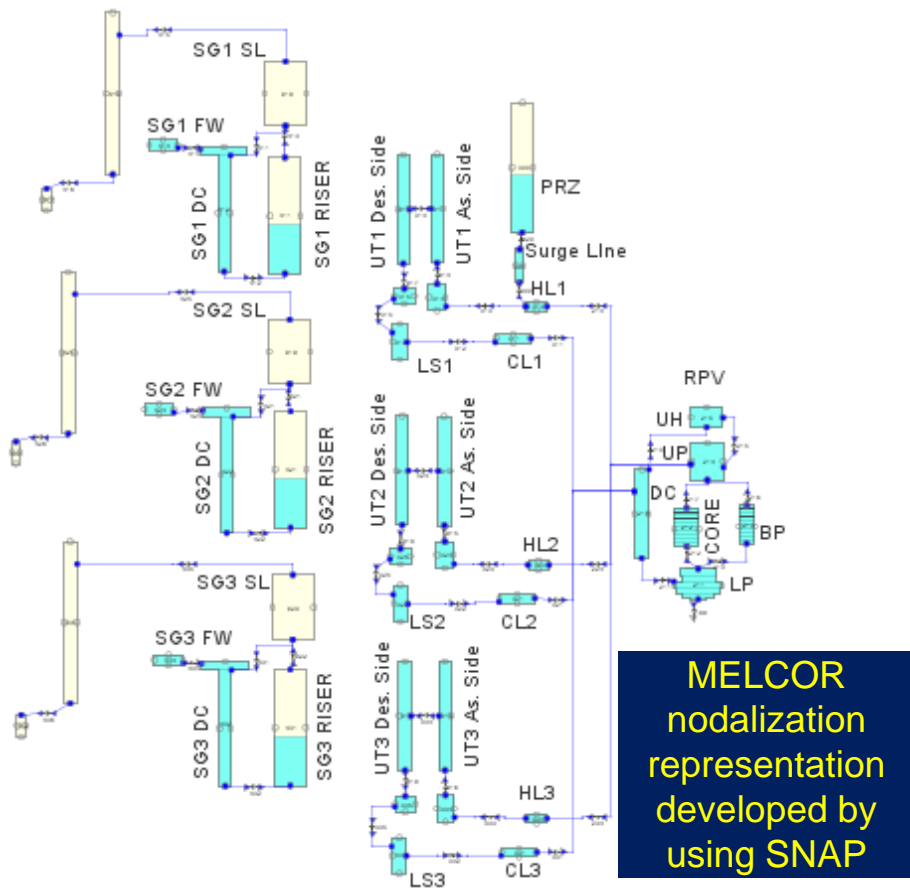


REF: <http://www.fauske.com/sites/default/files/MAAP5%20Primary%20System%20Nodalization%20Scheme.png>

CODE NODALIZATIONS: MAAP Plant Model Description-Containment

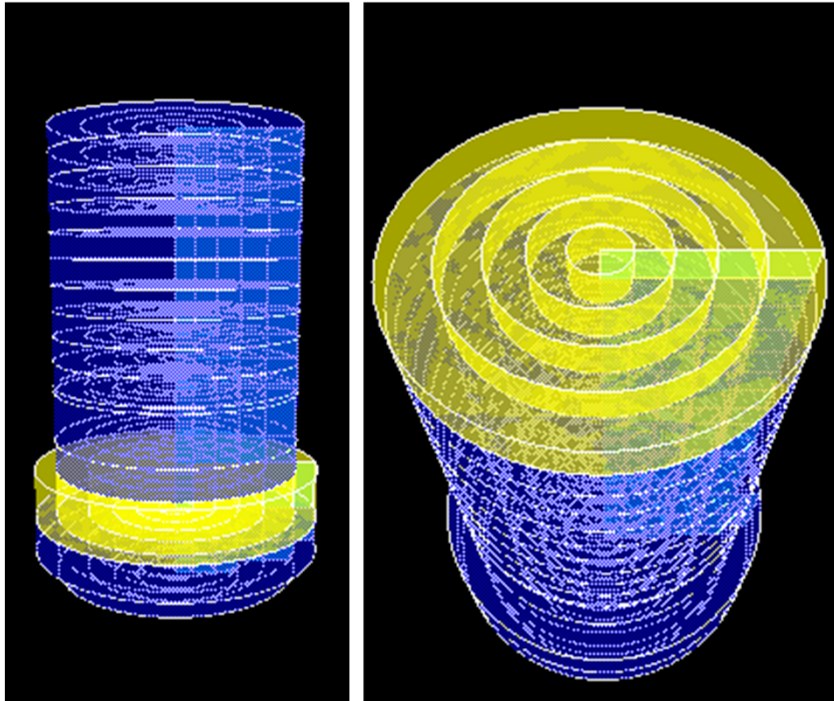


CODE NODALIZATIONS: MELCOR Plant Model Description



CODE NODALIZATIONS: MELCOR Plant Model

Description



MELCOR 3D core nodalization representation (COR package) developed by using SNAP

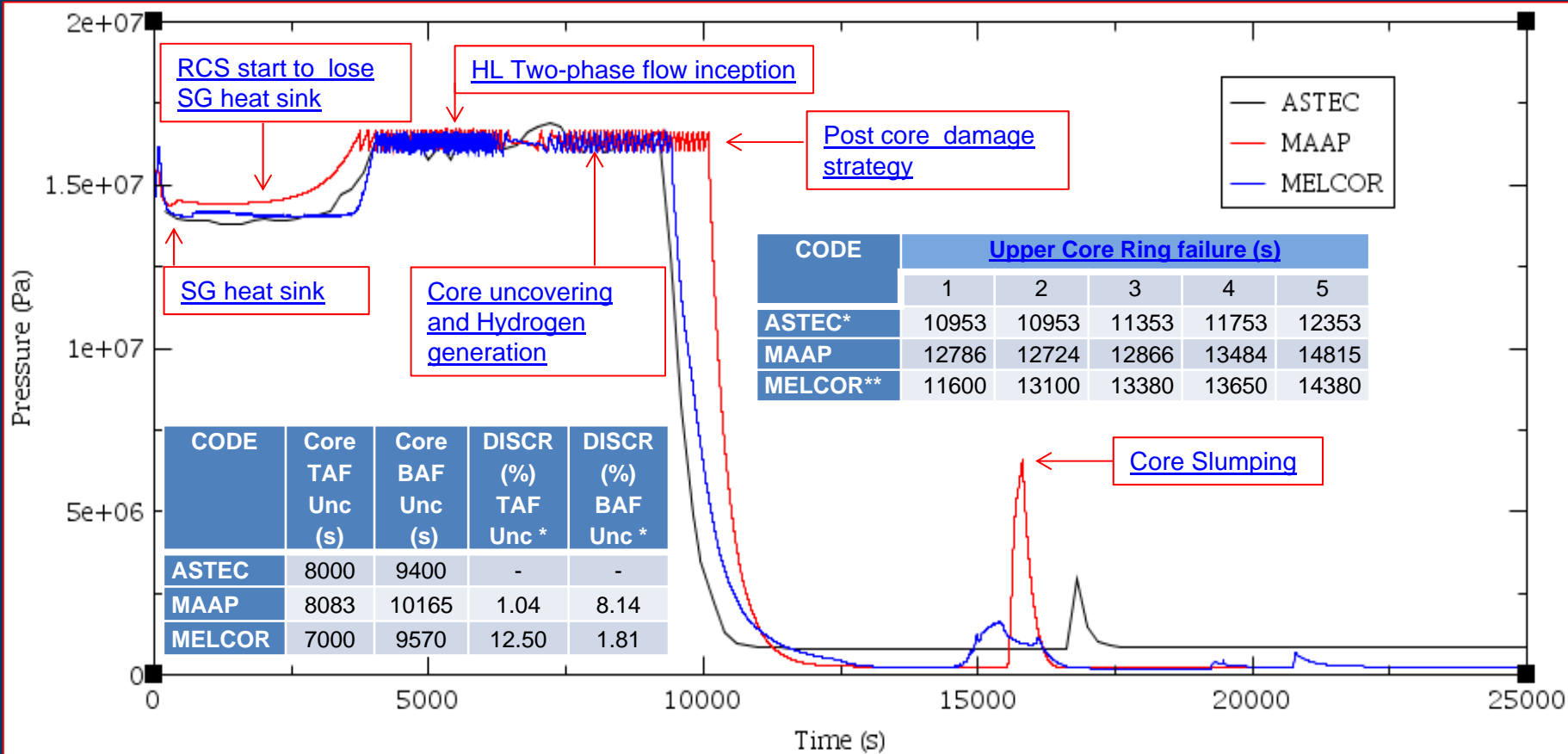
- Core is modelled by a single hydraulic region, CVH package, coupled with the correspondent MELCOR code model of the COR package.
- Core, in the COR package is modelled with 17 axial regions and 6 radial regions; 5 radial regions are used to model the core region (in agreement with ASTEC and MAAP nodalization).
- Lower plenum is modelled with 7 axial regions and the core with the remaining 10 axial regions.
- All supporting and non-supporting steel masses, Zircaloy masses, non-supporting Poison masses, and fuel Uranium masses are considered in the COR Package nodalization.
- 82.3 t of fuel and 19.23 t of Zircaloy are considered in the COR package.
- Lower head is composed of 13 rings with 10 lower head nodes.
- The candling heat transfer, the lower head failure modelling, the in-vessel falling debris quench model are activated. A hemisphere is used as a lower head type.



CODE CALCULATIONS: Steady State Analyses

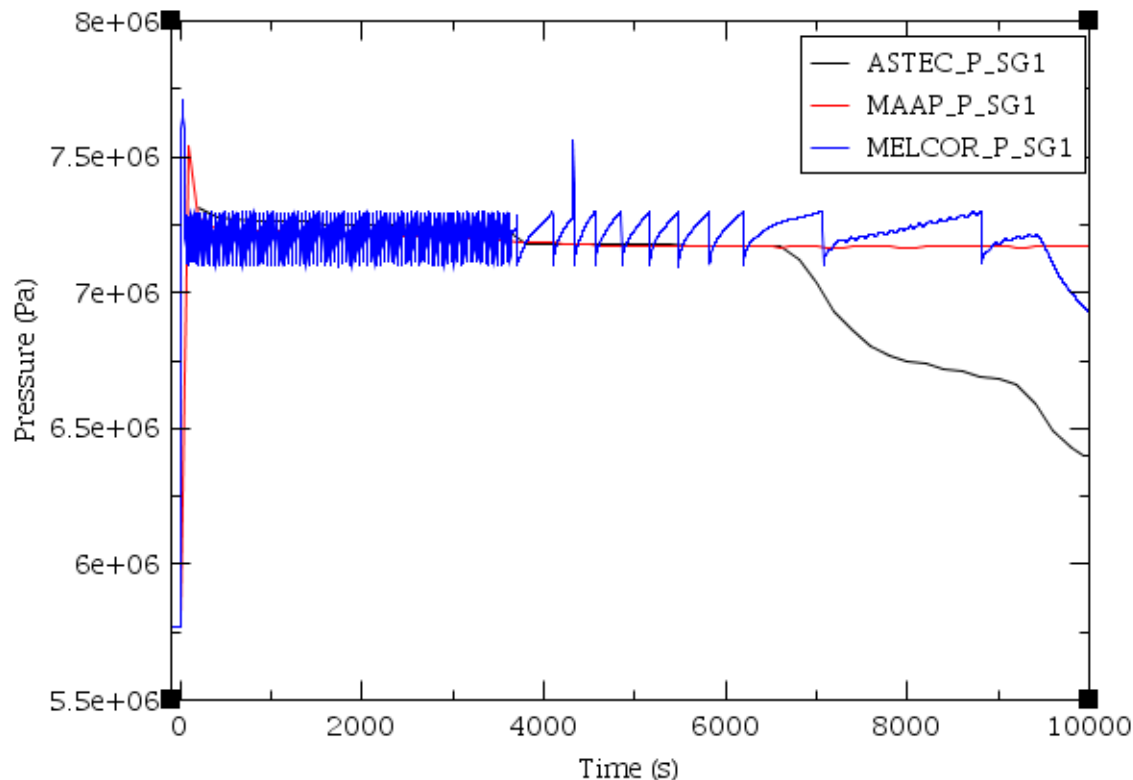
PARAMETERS	ASTEC	MAAP	MELCOR	MAAP DISCR(%)*	MELCOR DISCR(%)*
Primary side					
Pressurizer Pressure (bar)	155.16	155.89	154.78	0.47	0.24
Pressurizer Level (%)	50	49	50	2.00	0.00
Cold Leg 1 Flow Rate (kg/s)	4736	4738	4736	0.04	0.00
Core Flow Rate (kg/s)	13928	13894	13926	0.24	0.01
Upper Head Flow Rate (kg/s)	275	267	275	2.91	0.00
Primary Mass (kg)	185000	184535	185014	0.25	0.01
Inlet Core Temperature (K)	560	560	560	0.00	0.00
Outlet Core Temperature (K)	594.5	594.6	594.6	0.02	0.02
Secondary Side					
Separator Pressure (bar)	58	58	58	0.00	0.00
SG Water Mass (kg)	44385	44362	44385	0.00	0.00
SG Steam Mass (kg)	2725	-	2677	-	1.76
SG MFWS Flow Rate (kg/s)	512	-	512	-	0.00
Recirculation Ratio	4.15	4.15	4.15	0.00	0.00

**MAAP and MELCOR discrepancy (%) is calculated against the operational point predicted by ASTEC code.*



Primary pressure behaviour versus time

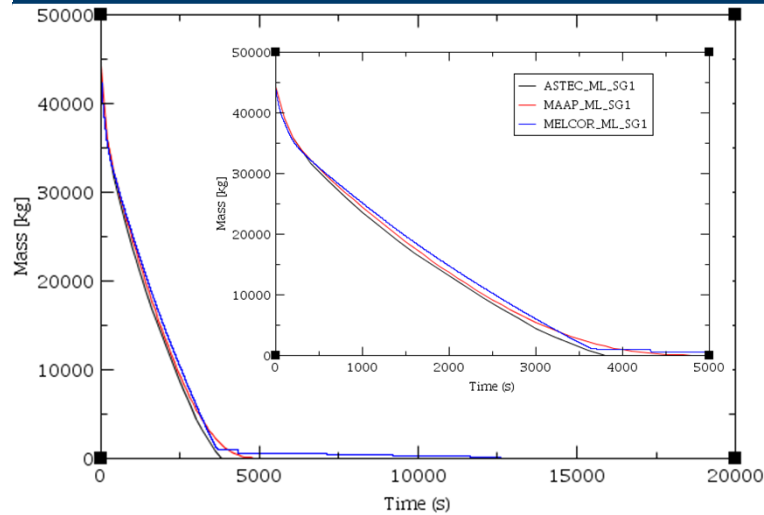
CODE CALCULATIONS: SG1 Secondary Pressure



- At the SOT the SGs remain the only heat sink of the residual power generated in the core.
- When the secondary side opening pressure set points are reached the SGs start releasing steam to the outside atmosphere.
- Cycling phase inception is predicted by all codes considering the different valve logics implemented in the three codes nodalization by the Code-Users.



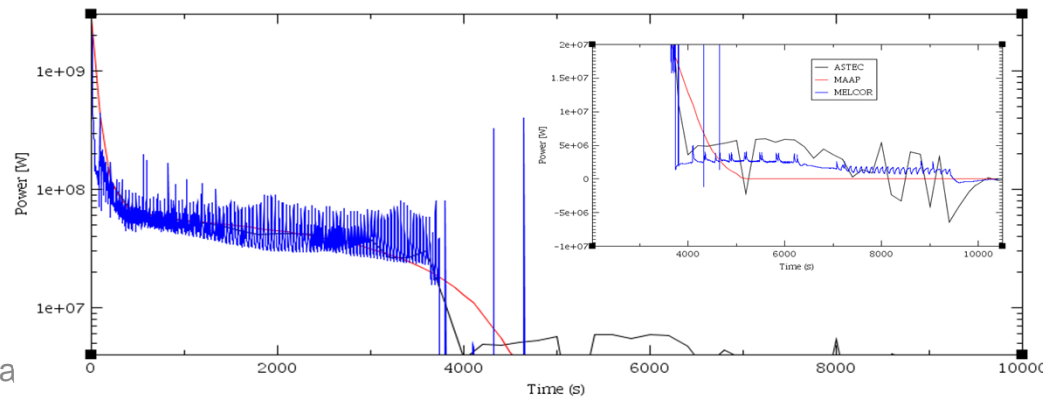
CODE CALCULATIONS: SG1 Liquid Mass and Total Heat Transfer Primary to Secondary Side



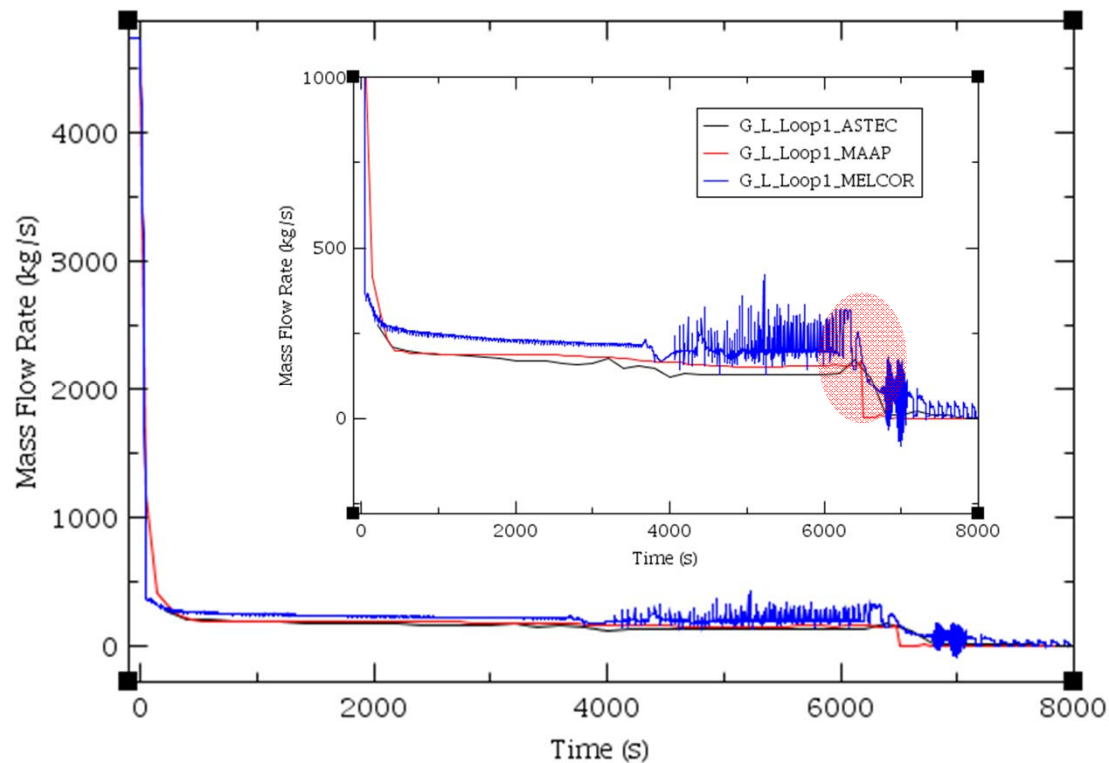
SG1 liquid mass inventory

- The SG opening and cycling determine a **SG mass inventory decrease**.
- After the secondary side **water depletion**, the decay heat transfer almost drops to negligible values

Total heat transfer between the primary to secondary



CODE CALCULATIONS: HL Loop1 Mass Flow Rate Versus Time



- Single-phase natural circulation in the primary side and heat transfer in a covered core are the main thermal-hydraulic phenomena characterizing this early phase of the transient in the primary side.
- All three codes predict the same qualitative behaviour even though some quantitative discrepancies are observed. In particular MAAP and MELCOR compute higher primary natural circulation mass flow rate compared with ASTEC code.
- When the two phase natural circulation starts a decrease in the mass flow rate is predicted by all codes.



CODE APPLICATION: Hydrogen Generation Characterization

CODE	H2 Start (s)	TCL 1300K (s) *	Heat up rate after T>1300 K (s)**	TCL 1855K (s) ***	In-Vessel H2 Max (s)	DISCR(%) diff H2 start ****	DISCR(%) TCL 1300K ****	DISCR (%) TCL 1855K ****	DISCR (%) H2 max ****
ASTEC	8400	9970	> 1 K/s	10080	17000	-	.	-	-
MAAP	8795	10845	> 1 K/s	10904	20876	4.7	8.8	8.2	22.8
MELCOR	8382	8700	> 1 K/s	9248	19250	0.2	12.7	8.3	13.2

**For ASTEC code the second ring behaviour is analysed, because it is the faster to increase the cladding T; for MAAP code the second ring behaviour in the upper part of the core is analysed (axial = 58/radial =1), because it is the faster to increase the cladding T; for MELCOR code the first ring behaviour at the 8th core level is analysed because it is the faster to increase the cladding T (the core is modelled by using 10 axial level).*

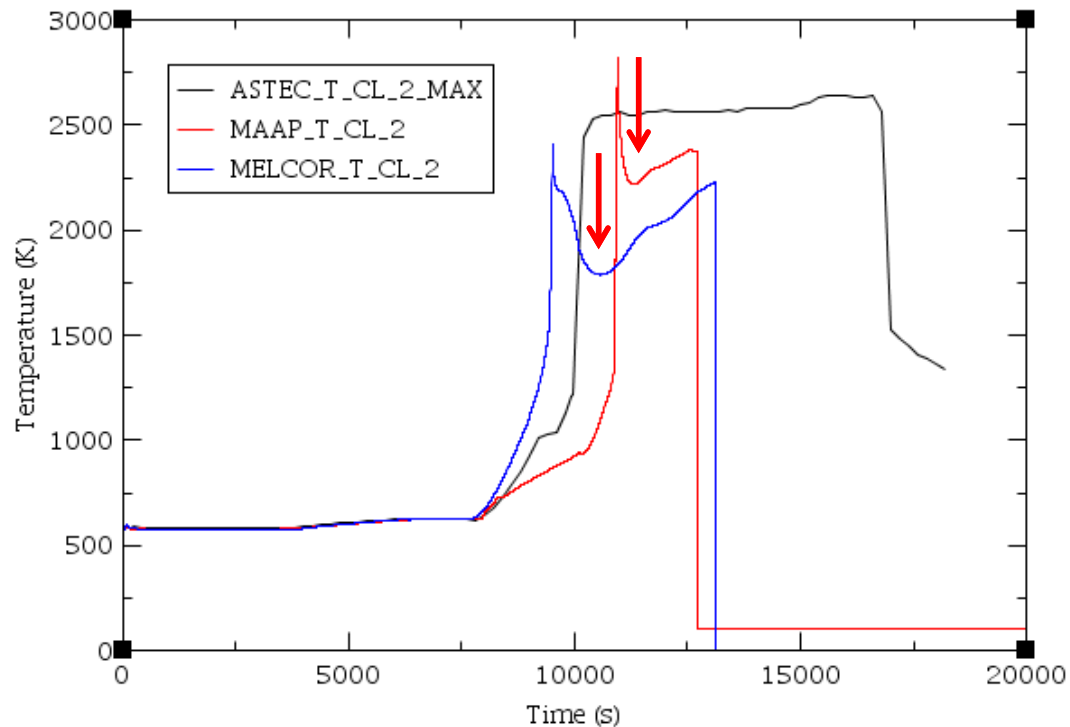
*** The heat up rate is an important parameter because permits the operator actions and influences the phenomenology of oxidation and liquid formation in the core.*

****For ASTEC code the second ring behaviour is analysed, because it is the faster to increase the CL T; for MAAP code the second ring behaviour in the upper part of the core is analysed (axial = 58/radial =1), because it is the faster to increase the CL T; for MELCOR code the first ring behaviour at the 8th core level is analysed because it is the faster to increase the cladding T.*

***** ASTEC calculated data discrepancies based on the comparison with MAAP and MELCOR calculated data.*



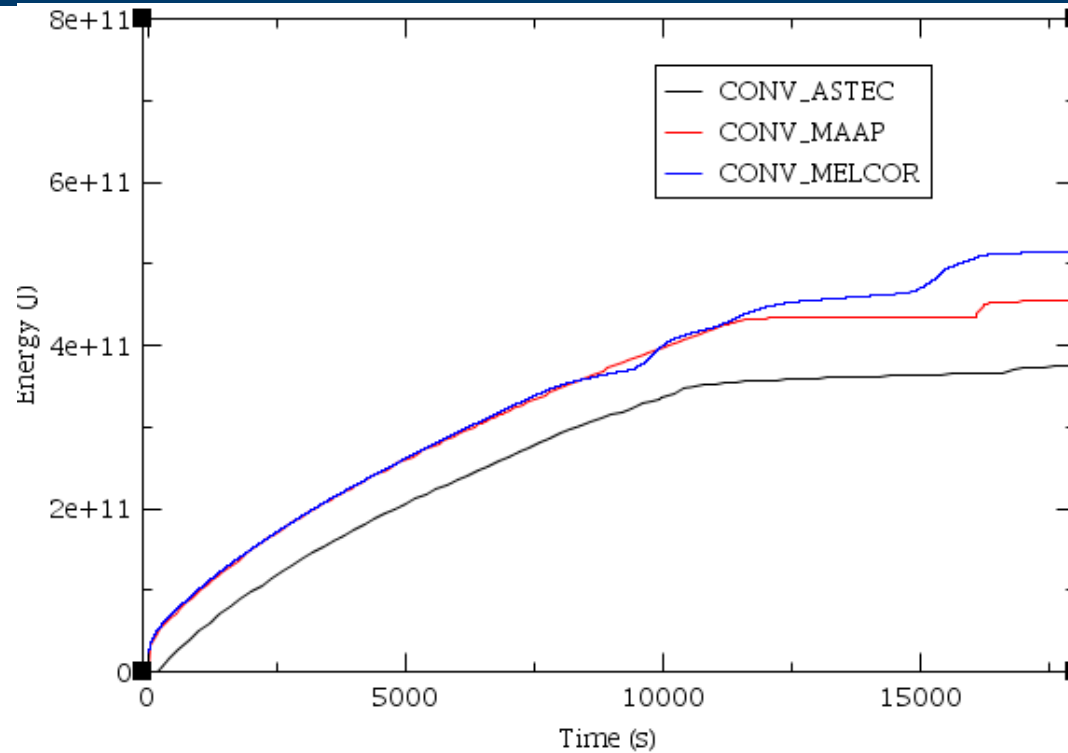
CODE CALCULATIONS: Cladding Temperature



Intact cladding temperature at the 2th ring in the upper part of the core predicted by MAAP and MELCOR code and max intact cladding temperature of the ring 2 predicted by ASTEC

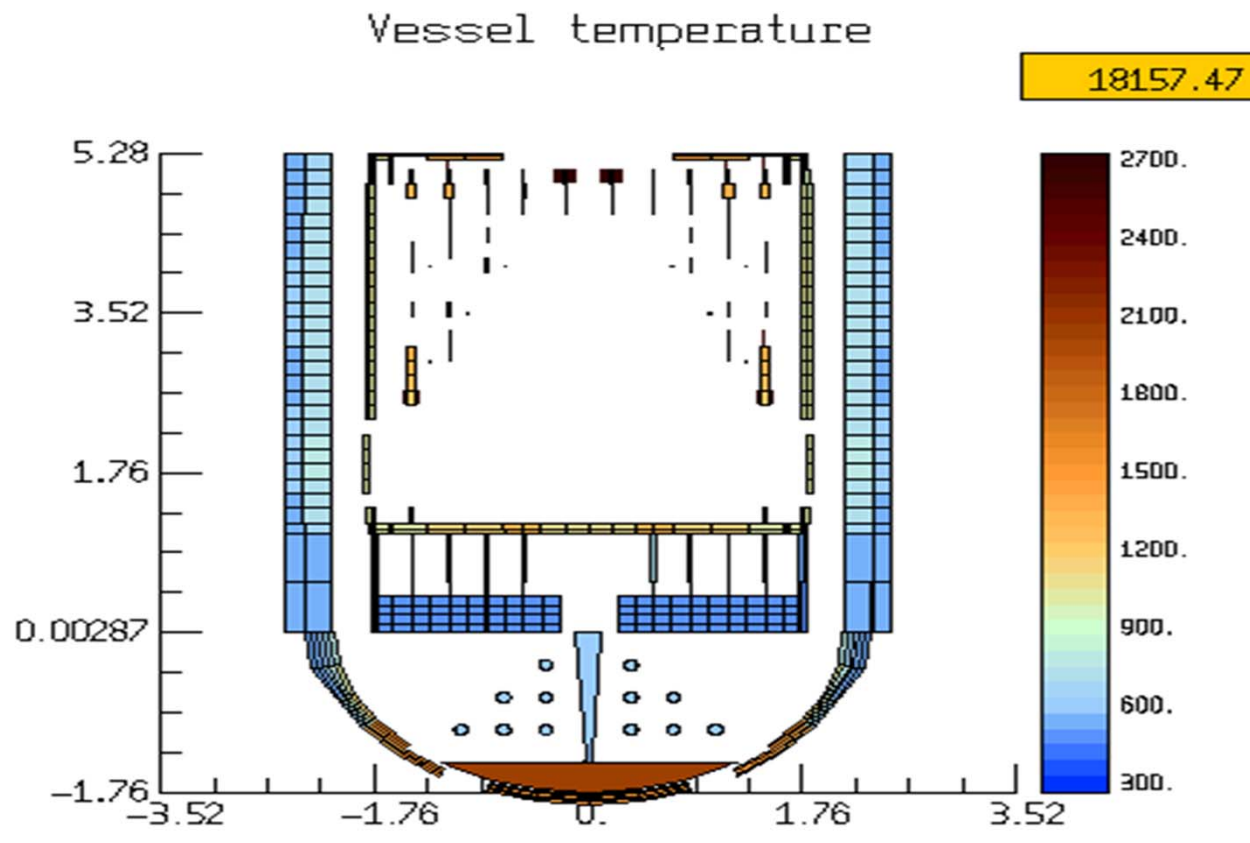
- In MAAP a **first clad temperature peak** (rings 2,3,4), more pronounced in the ring 2, is followed by a **cladding temperature decrease** following by a further cladding temperature increase.
- The intact cladding temperature decrease could be due to a **formation of a two phase flow in the core due to the SEBIM valve stuck opening**.
- The same phenomenon is observed in MELCOR code.
- **MELCOR code removes more energy in comparison with MAAP** starting from 9908s after the SOT. This could be one of the reasons of the more sensible reduction of cladding temperature in the MELCOR calculation.

CODE CALCULATIONS: Energy Removed by the Fluid

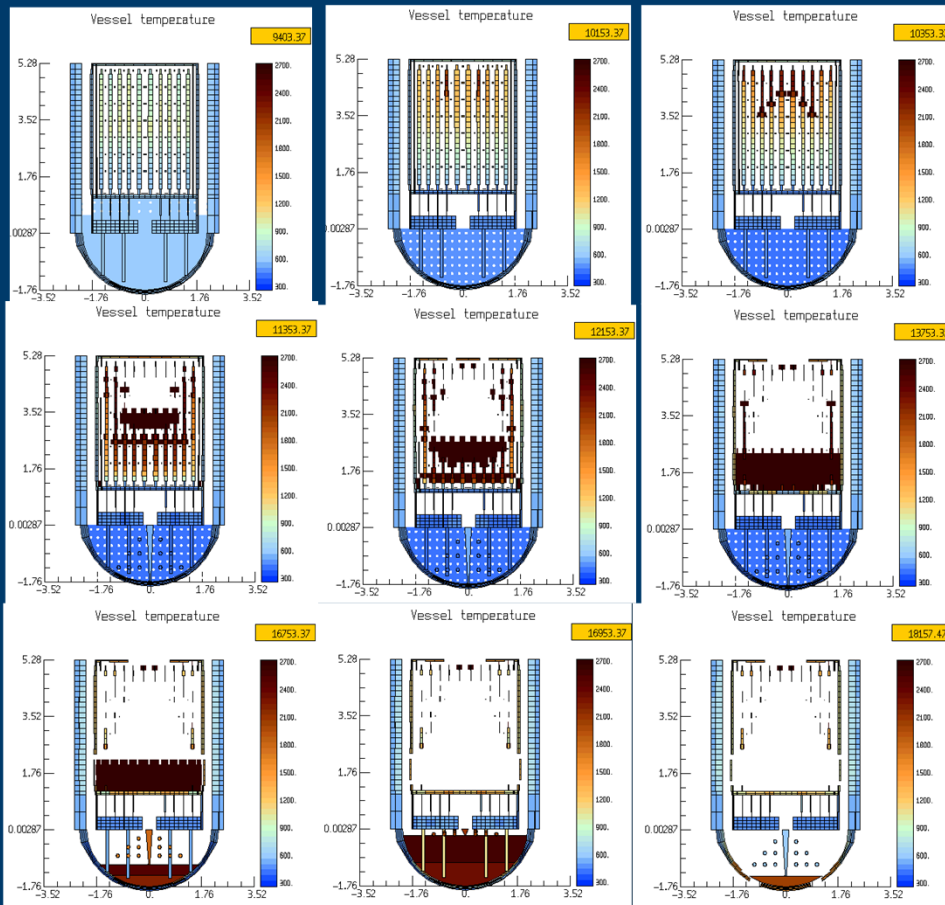


ASTEC evolution is not quantitatively representative because the data are available (from the code user) from 200s after the SOT and the integration of the power data- available from ASTEC- is missing during the first 200s)



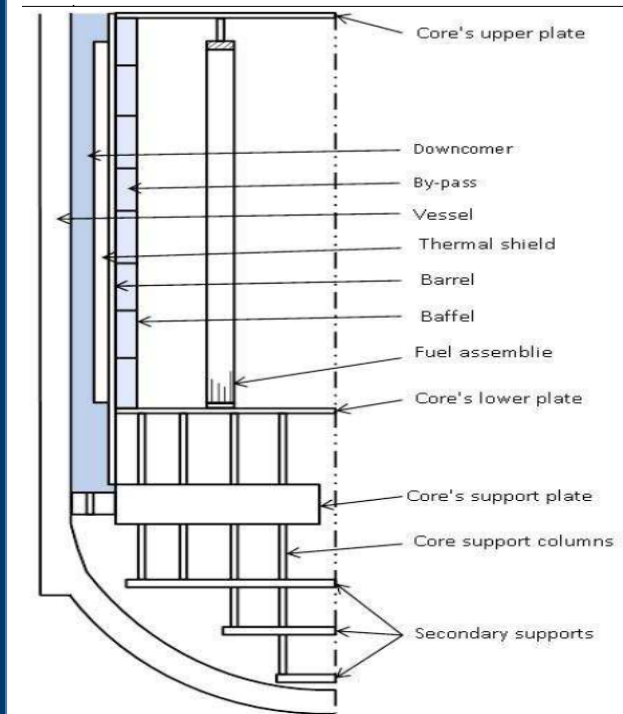
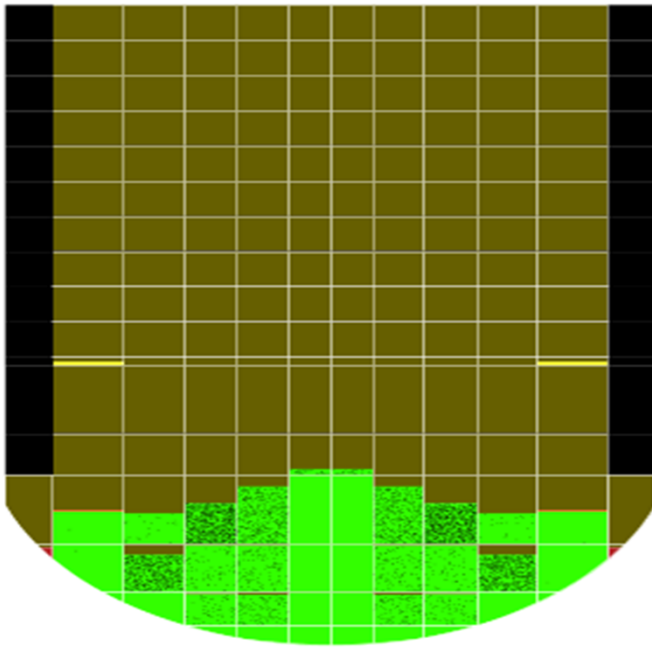


ASTEC Core Degradation Visualization



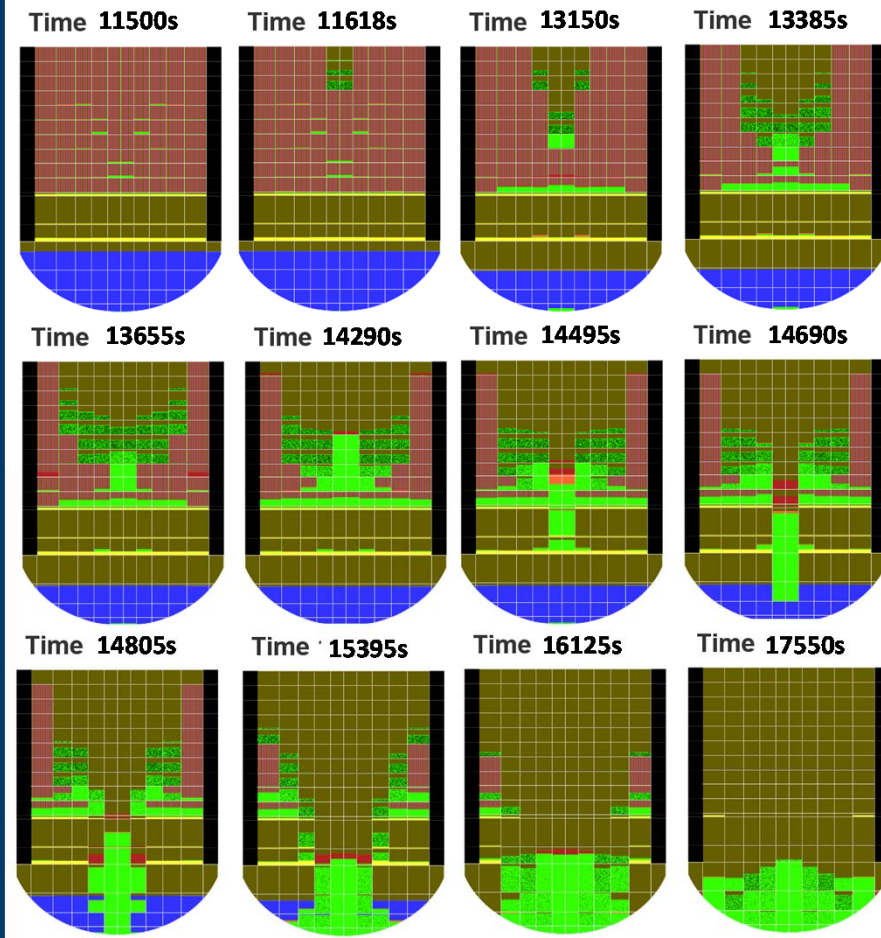
ASTEC Core Degradation Visualization Selected Instants

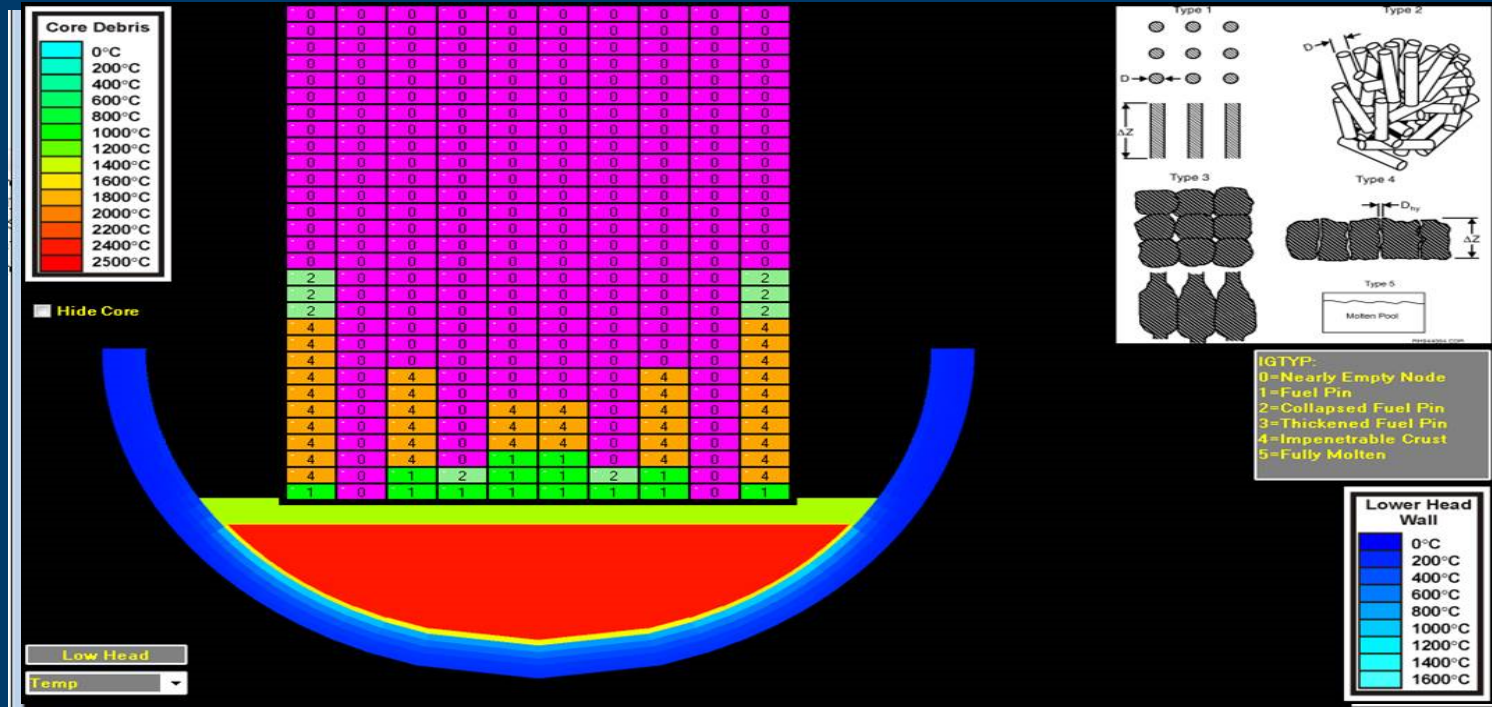
Time 17550s



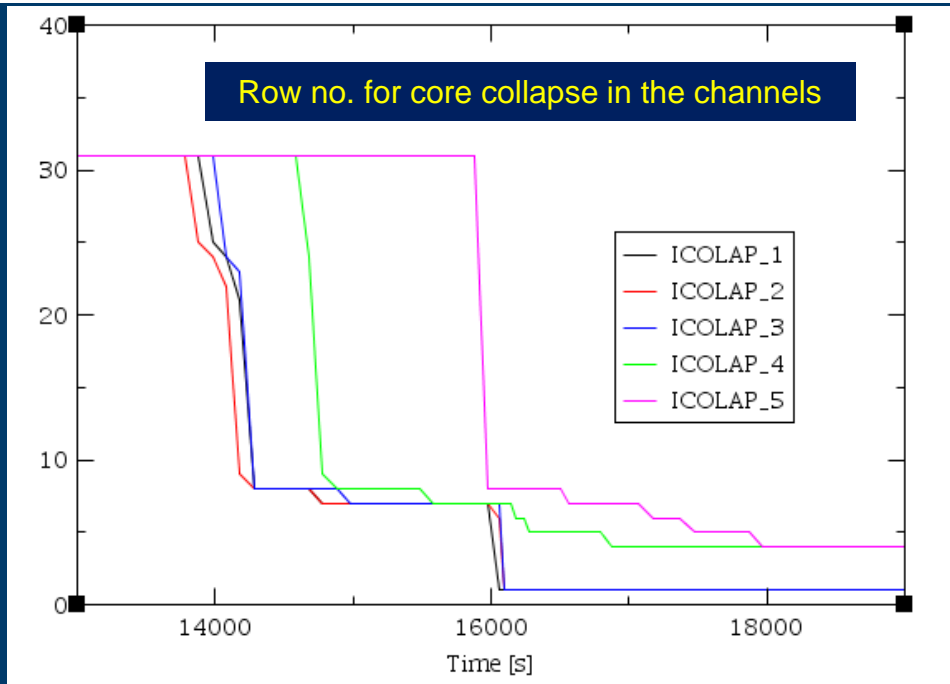
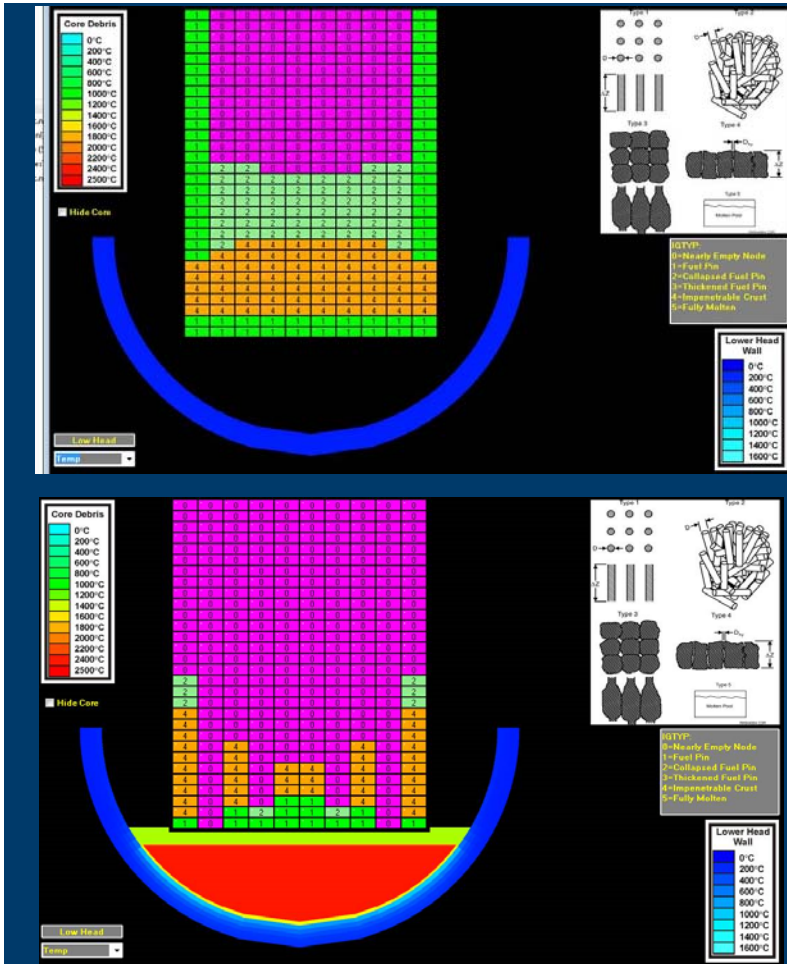
MELCOR Core Degradation Visualization by Using SNAP

MELCOR Core Degradation Visualization, by Using SNAP, Selected Instants





MAAP Core Degradation Visualization



MAAP Core Degradation Visualization selected instants

CODE CALCULATIONS: Core Relocation

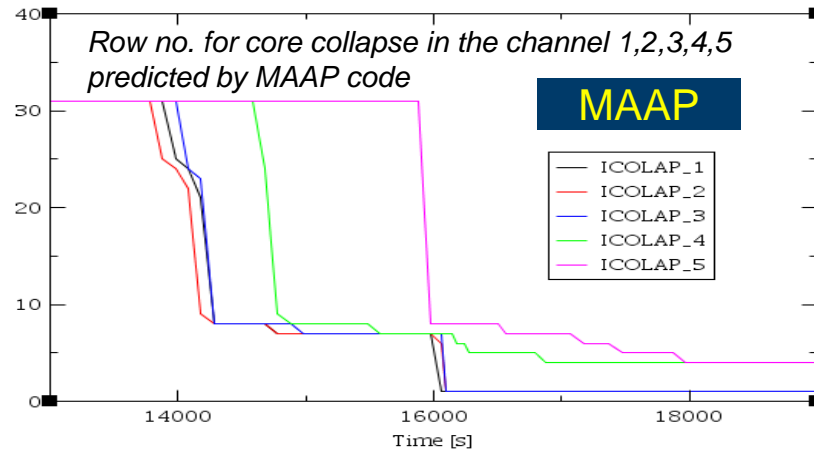
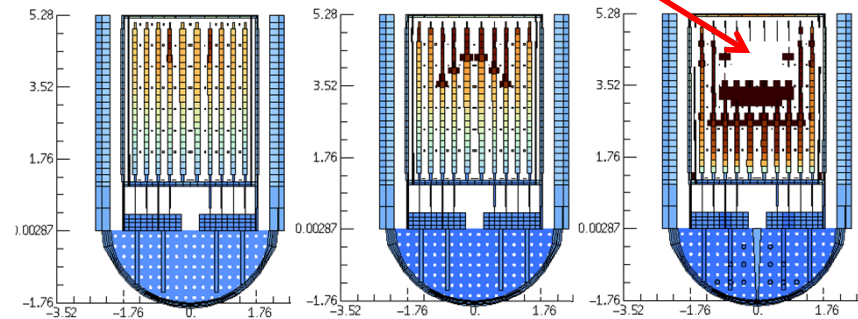
CODE	Upper Core Ring failure (s)				
	1	2	3	4	5
ASTEC*	10953	10953	11353	11753	12353
MAAP	12786	12724	12866	13484	14815
MELCOR**	11600	13100	13380	13650	14380

*Considering previous figure, where ASTEC core degradation/relocation visualization is reported, instead of considering the upper core ring failure, it is estimated the instant when the fuel ring continuity is lost.

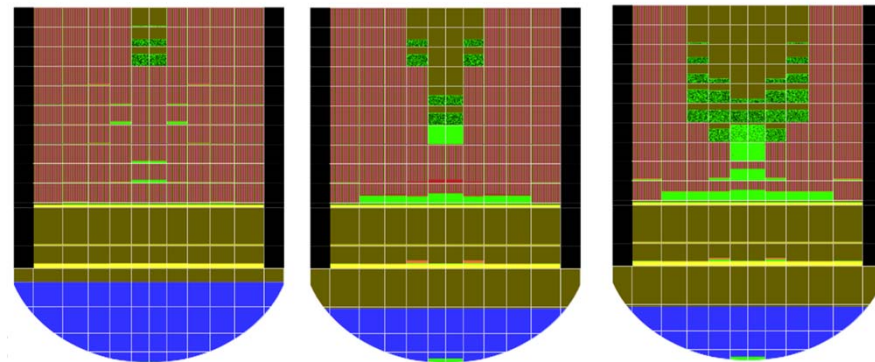
** Upper part of the 5th ring starts to collapse at 14380s, but other axial levels continue their failure starting from 15270s.

fuel ring continuity is lost

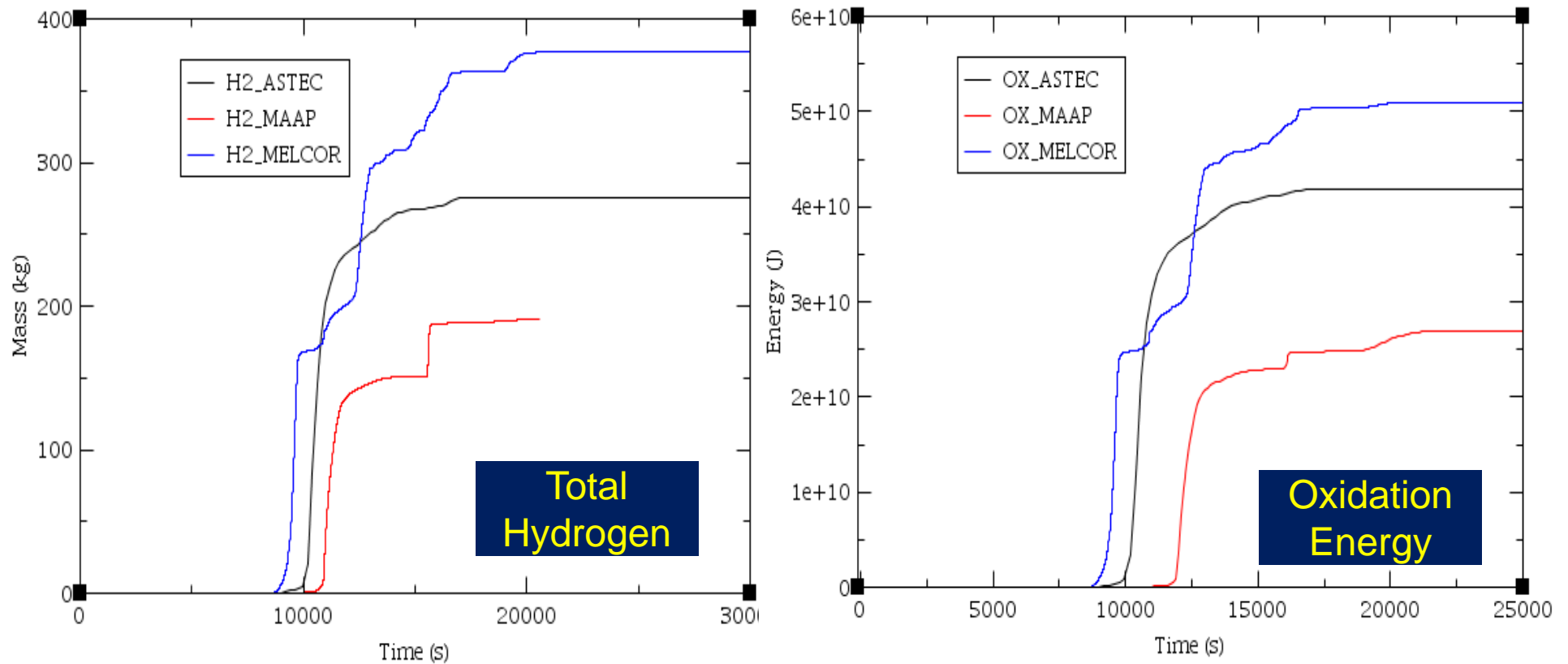
ASTEC



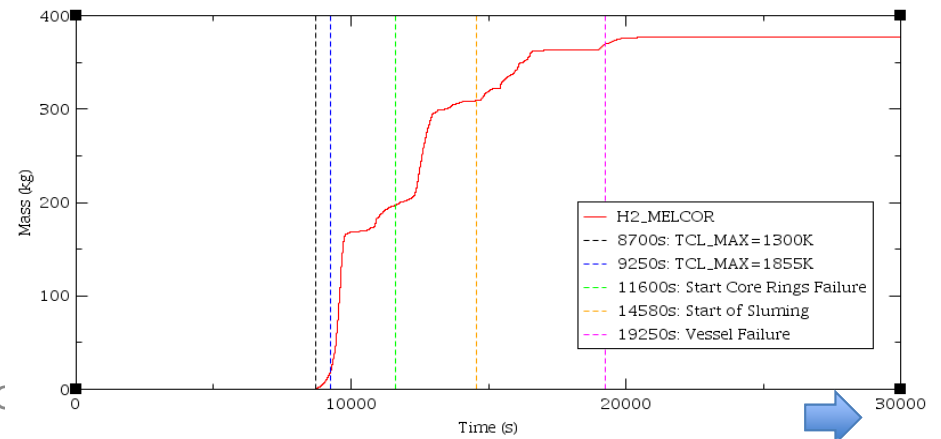
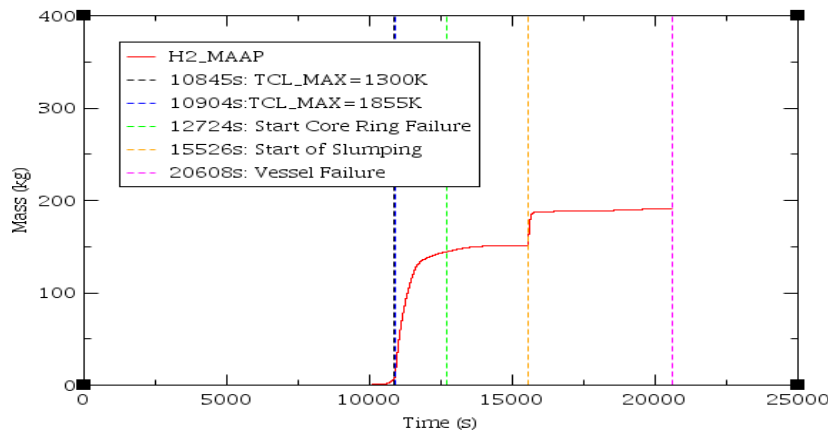
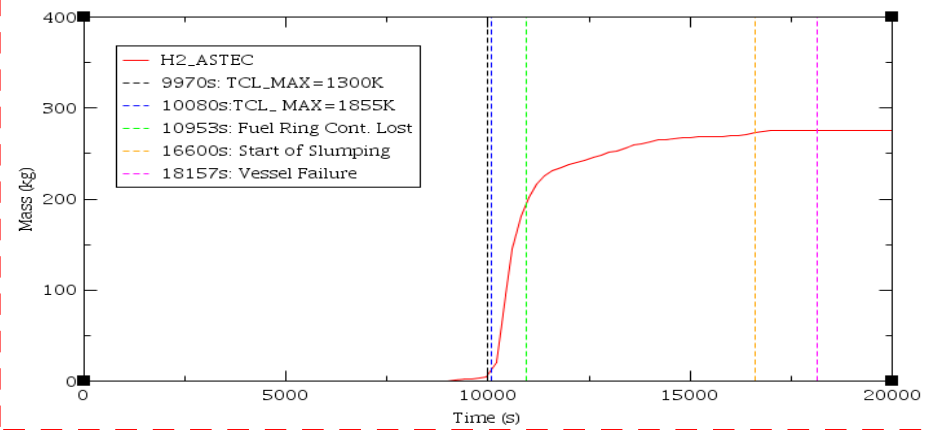
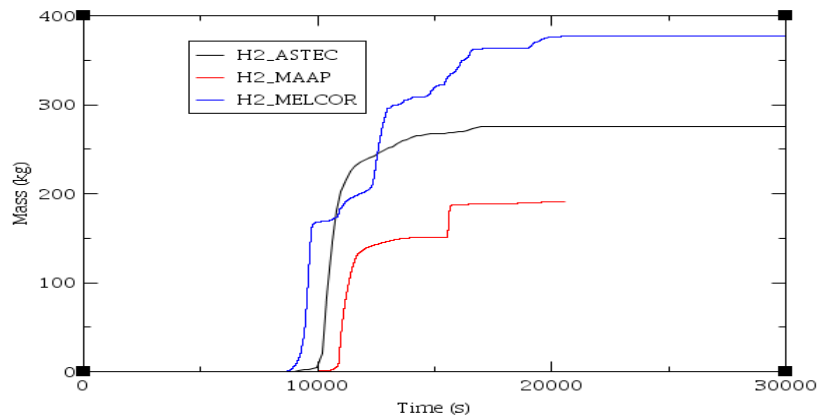
MELCOR



CODE CALCULATIONS: Total Hydrogen Generation/Oxidation Energy Generated in the Core



CODE APPLICATION: Hydrogen Generation Characterization



User (

CODE CALCULATIONS: Hydrogen Generation and Core Relocation

- The materials with a lower melting temperature than fuel (as control rod, guide tube, grids.....) determine the **starting of the melting and relocation phase of the core damage**.
- Along the core degradation and melt progression phase, the **cladding and fuel failure mechanisms and the consequent core materials transport/relocation take place**.
- These phenomena **determine a loss of core geometry with a consequent change of the coolant flow path shape**.
- The hydrogen mass production is therefore dependent from the core degradation progression and the consequent **available area for the oxidation and flow blockage phenomena**.
- Though the uncertainty to correctly estimate the amount of **area available and the effect of flow blockage**, in general a significant amount of hydrogen could be produced during this phase of the transient and it is estimated by the codes **considering their different core material degradation/relocation modelling capability**.

CODE CALCULATIONS: Hydrogen Generation and Core Relocation

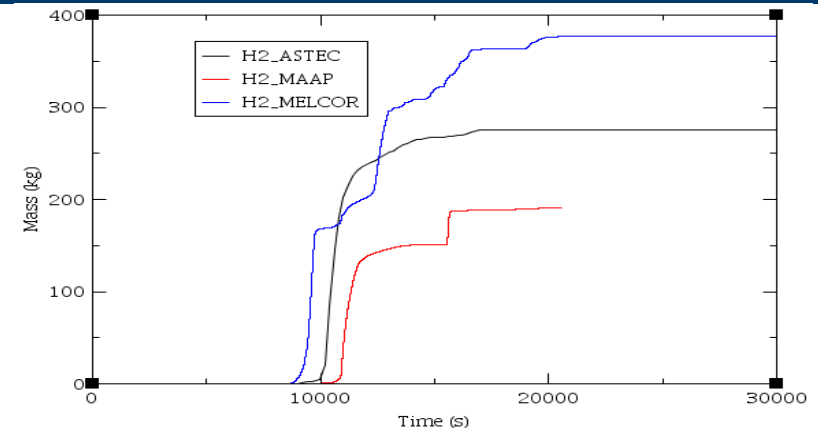
- Though a detail characterization and analyses of the core material relocation/distribution and the codes representation is out of the target of the research activity here presented, the macroscopic effect of the hydrogen generation is here analysed.
- **ASTEC** code shows a **general smooth progressive hydrogen production** along the core degradation phase.
- **MAAP** code shows a **general smooth progressive hydrogen production**.
- MELCOR code shows instead a **general progressive hydrogen production**, but the previous mentioned stuck opening of the SEBIM valve determines a sensible reduction and a subsequent increase (when the cladding temperature increase again) of the oxidation rate. This, coupled with the progressive upper ring core failure and the progressive relocation of the core in the lower plenum, determines the hydrogen production versus time behaviour.



CODE CALCULATIONS: Hydrogen and Slumping

CODE	H2 Before Slumping (Kg)	Tot In Vessel H2 (Kg)	DISCR (%) Before Slump*	DISCR (%) H2 TOT *
ASTEC	273	275	-	-
MAAP	151	191	44.69	30.55
MELCOR	309	377	13.18	37.09

*ASTEC calculated data discrepancies based on the comparison with MAAP and MELCOR calculated data.



- After the core material relocation into the lower plenum (slumping) **additional hydrogen could be generated** due to the oxidation phenomena;
- This part of the transient is strongly influenced by the core relocation scenario;
- **While in MELCOR and MAAP code the slumping takes place through the core plate failure, in ASTEC code it takes place due to the failure of the shroud;**
- In ASTEC, the hydrogen production is characterized by a very small increase that permits to conclude that **all the hydrogen is created before the slumping.**

CODE CALCULATIONS: Hydrogen Generation

- Hydrogen mass production is dependent on the core degradation progression and:
 - the consequent available area for the oxidation;
 - flow blockage phenomena.
- Discrepancies related to these parameters underline the modelling difference of the code related to core material degradation/relocation determining:
 - differences in the available area for the oxidation process,
 - different flow blockage condition, and
 - differences in the code node porosity predicted, etc.
- It is important to underline that the **area available for the oxidation has a great uncertainty** due to the complex phenomena taking place during the degradation and relocation of the core material and limited full scale experiments.

CODE CALCULATIONS: Transient Analyses

RELEVANT PHENOMENOLOGICAL ASPECTS	ASTEC	MAAP	MELCOR	MAAP DISCR* (%)	MELCOR DISCR* (%)
SG1,2,3 Cycling Inception (s)	200	100	30	-	-
SEBIM Cycling Inception (s)	4200	3757	4058	10.55	3.38
Two Phase inception in the HL (s)	6400	6404	6300	0.06	1.56
Core TAF Uncovered (s)	8000	8083	7000	1.04	12.50
H2 Start (s)	8400	8795	8382	4.70	0.21
SEBIM Stuck Open (s)	9200	10099	9414	9.77	2.33
Core BAF Uncovery (s)	9400	10165	9570	8.14	1.81
TCL 1300K (s)	9970	10845	8700	8.78	12.74
TCL 1855K (s)	10080	10904	9248	8.17	8.25
Upper Core Ring Failure 1 (s)**	10953	12786	11600	16.74	5.91
Upper Core Ring Failure 2 (s)**	10953	12724	13100	16.17	19.60
Upper Core Ring Failure 3 (s)**	11353	12866	13380	13.33	17.85
Upper Core Ring Failure 4 (s)**	11753	13484	13650	14.73	16.14
Upper Core Ring Failure 5 (s)**/**	12353	14815	14380	19.93	16.41
Slumping Inception (s)	16600	15526	14580	6.47	12.17
Vessel Failure (s)	18157	20608	19250	13.50	6.02

**ASTEC calculated data discrepancies based on the comparison with MAAP and MELCOR calculated data.*

***For ASTEC it is estimated the instant when the fuel ring continuity is lost.*

*** For MELCOR calculation, the upper part of the 5th ring starts to collapse at 14380s, but other axial levels continue their failure starting from 15270s.*

CONCLUSIONS

- ❑ The results of the calculated data show that the **three codes predict the phenomenological evolution in a good qualitative agreement even though with some quantitative differences.**
- ❑ In particular, considering the time sequence of relevant phenomenological aspects, the maximum percentage discrepancy between ASTEC and MAAP/MELCOR calculated data is at maximum of about 20% for the main selected safety related parameters chosen as figure of merit.
- ❑ **The most relevant differences are observed in the in-vessel hydrogen mass production prediction.** Such discrepancies underline some modelling differences between the three codes related to core material degradation/relocation, determining differences in the available area for the oxidation process, different flow blockage conditions, different code node porosity prediction, etc.
- ❑ **In addition, it is worth noting a phenomenological discrepancy related to the slumping predictions between ASTEC and MAAP/MELCOR calculations:** while MAAP and MELCOR predict a core lower plate failure with a consequent relocation of degraded core material in the lower plenum, ASTEC predicts the relocation of the degraded core material through the shroud failure.


CONCLUSIONS

□ Considering:

- the hypotheses of the transient (no ECCS intervention, scram at zero, no pump leakage, etc)
- the maximum degree of freedom left to the *Code-User* (hydraulic and core nodalization strategy and degree of detail, setting of the boundary condition...)
- the general phenomenological agreement of the transient phenomenology predicted by the three codes (with the exception of the slumping phenomenology)

the results of the **code calculations can be used as a confirmation of the transient phenomenological evolution of the postulated accident.**

- ## □ Future activity based on a **strictly congruence analysis between core structures nodalizations (geometry and mass) is endorsed.**



Authors thank the funding received from the 7th Framework Programme of the European Commission via the CESAM project;

Special thanks to GRS for the coordination of Project;

Special thanks to JRC for the coordination of the WP2.3 activities;

Special thanks to IRSN for the support and comments on the activity.